December 2018

In Vivo Analysis of Pedf Expression in the Prostate, Liver, and Adipose Tissue in Obese Microenvironments

Samantha Woller
University of Wisconsin-Milwaukee

IN VIVO ANALYSIS OF PEDF EXPRESSION IN THE PROSTATE, LIVER, AND ADIPOSE TISSUE IN OBESE MICROENVIRONMENTS

by

Samantha Woller

A Thesis Submitted in

Partial Fulfillment of the

Requirements for the Degree of

Master of Science

in Biomedical Sciences

at

The University of Wisconsin- Milwaukee

December 2018

ABSTRACT

IN VIVO ANALYSIS OF PEDF EXPRESSION IN THE PROSTATE, LIVER, AND ADIPOSE TISSUE IN OBESE MICROENVIRONMENTS

by

Samantha Woller

The University of Wisconsin – Milwaukee, 2018
Under the Supervision of Jennifer A. Doll, PhD

Prostate cancer is the second most common form of cancer among males in the United States. An association has been established between aggressive prostate cancer and obesity. The obese microenvironment can promote tumor growth. The *Serpinf1* gene encodes pigment epithelium-derived factor (PEDF), a tumor suppressor gene which has anti-angiogenesis and direct anti-tumor properties. Notably, expression of this protein is suppressed in prostate cancer cells. Our lab has previously demonstrated further suppression of PEDF expression within a prostate epithelial cell line and prostate cancer cell lines *in vitro*, when the cells were grown in an obese microenvironment. The experiments outlined in this study were conducted to determine if PEDF expression is suppressed *in vivo*, in prostate, liver, and periprostatic adipose tissue in an obese microenvironment. It was hypothesized that the PEDF levels would be lower in the prostate tissues and periprostatic adipose tissue, but higher in liver tissue in the obese microenvironments. *In vivo* experiments were conducted using two different obesity

models, (A) wild-type C57BL/6 mice on a control diet (CD) or a high fat diet (HFD) and (B) wild-type and Ob/ob strains of C57BL/6 mice on a standard laboratory diet. All experimental diets began at 8 weeks of age and were carried out for 16 weeks. Prostate, liver, and adipose tissues were harvested when mice were 6 months old. Protein levels in tissue homogenates were analyzed with a Coomassie assay. Then, PEDF protein levels were quantified with an ELISA. In the majority of samples, no significant difference in PEDF levels was found when comparing the HFD or ob/ob mice to their respective control group. One difference was observed within the anterior prostate lobe in the ob/ob mice. This experiment also suggested that there are higher levels of PEDF in the ventral prostate lobe in the WT control mice when compared to the anterior and dorsolateral prostate lobes. These are the first reported data of PEDF levels in both the prostate and periprostatic adipose tissue in mice. While these data, overall, did not support the hypothesis, due to large variances in PEDF levels, further studies are needed to confirm that an obese microenvironment does indeed have no effect on PEDF levels in prostate, liver, and adipose tissue *in vivo.*

Table of Contents

List of Figures

List of Tables

List of Abbreviations

5-Aza-dC	5-aza-2-deoxycytidine
5mC	5-methylcytosine
ASC	Adipose Stromal Cells
BMI	Body Mass Index
BPH	Benign Prostatic Hyperplasia
CCL7	C-C Motif Chemokine Ligand 7
CCR3	C-C Motif Chemokine Receptor
CD	Control Diet
CGI	CpG Island
ChIP-seq	Chromatin Immunoprecipitation Analysis and Sequencing
CHOP	CCAAT/Enhancer Binding Protein
CRPC	Castration Resistant Prostate Cancer
CXCL1	C-X-C Motif Ligand 1
CXCL8	C-X-C Motif Ligand 8
CXCR1	C-X-C Motif Receptor 1
CXCR2	C-X-C Motif Receptor 2
DNMT	DNA Methyltransferases
ELISA	Enzyme-Linked Immunosorbent Assay
Foxa1	Forkhead Box A1
Foxa2	Forkhead Box A2
HFD	High Fat Diet

HNF4	Hepatocyte Nuclear Factor 4
LOX-1	Lectin-like Oxidized Low-Density Lipoprotein Receptor 1
MBD2	DNA demethylase
mCRPC	Metastatic Castration-Resistant Prostate Cancer
miRNA	Micro RNA
MITF	Microphtalmia-Associated Transcription Factor
NCoR1	Nuclear Receptor Co-Repressor
NS	Non-significant
OA	Oleic Acid
oxLDL	Oxidized Low-Density Lipoprotein
PEDF	Pigment Epithelium-Derived Factor
Phlda1	Pleckstrin Homology Like Domain Family A Member 1
PITX1	Paired-like Homeodomain 1
PMSF	Phenylmethane Sulfonyl Fluoride
PSA	Prostate Specific Antigen
RPE	Retinal Pigment Epithelial
TFPI2	Tissue Factor Pathway Inhibitor 2
TSA	Trichostatin A
USF	Upstream Stimulatory Factor 1
WAT	White Adipose Tissue
WT	Wild-Type

INTRODUCTION

Prostate Cancer

Prostate cancer is the second most common cancer among males in the United States; one out of every eight men in the United States will be diagnosed with prostate cancer in their lifetime [1]. An estimated 164,690 new cases of prostate cancer will be diagnosed in 2018 and 29,430 deaths are expected to occur due to the disease [2]. Prostate cancer most commonly causes urinary problems including weak or frequent urination, difficulty urinating, sudden urge to urinate, dysuria, and hematuria, and may also cause blood in semen or lower back, hip, or pelvic pain [1].

Prostate cancer can be detected in various ways including a digital rectal exam, prostate-specific antigen (PSA) testing, and transrectal imaging. Its presence is confirmed by biopsy and pathological analysis [1]. Prognosis and treatment options are dependent on the stage of the cancer, tumor grade, and other factors including the patient's age. Common treatments for prostate cancer include prostatectomy, transurethral resection, radiation, chemotherapy, hormone ablation, and active surveillance. Prostatectomy and radiation therapies are effective in the short term; however, approximately 30% of patients will experience clinical recurrence noted by elevated PSA levels (biochemical recurrence) and/or detection of distant metastasis [3]. As a primary, or as adjuvant, treatment androgen deprivation therapies are also utilized due to the fact that prostate cancer development and progression is dependent on androgens. Yet again, this course of treatment is not effective long-term. While the treatment initially is quite effective in suppressing androgen function and tumor growth, the therapy typically exerts effects for a

maximum average of 24 months [3]. Within those 24 months, it is common for the disease to progress into castrate-resistant prostate cancer (CRPC) in which the cancer is able to grow even in with low amounts of circulating androgens [4]. While these treatment options can extend life, a lasting cure for metastatic castrate-resistant prostate cancer (mCRPC) has yet to be discovered.

Furthermore, the risk of developing prostate cancer increases significantly with age and is rarely seen in men younger than 40 [1]. The probability of a man under the age of 49 being diagnosed with prostate cancer is 1 in 354, but in men over the age of 70, the probability escalates to 1 in 11 [1]. About 10% of prostate cancer diagnoses are in men under the age of 56, which is considered early-onset prostate cancer; however, this number appears to be on the rise, increasing nearly 6-fold from 1986 to 2008 [5, 6]. A population-based cohort study revealed that the proportion of early-onset diagnoses increased from 3.9% between 1988 and 1991 to 10.9% between 2000 and 2003 [6]. The authors propose that this rise may be due to evolving screening and treatment techniques. They also note that men who developed early-onset prostate cancer were less likely to be diagnosed with organ-confined tumors, but also were less likely to develop high-grade cancer for reasons unknown at this time [6]. Studies suggest that there may be biological differences and a stronger genetic component when compared to later onset prostate cancer [5]. Family history of prostate cancer, race, androgen levels, high fat diet (HFD), and obesity also affects an individual's risk [1] .

Prostate Cancer and Obesity

Obesity, specifically as a risk factor of prostate cancer, is of great concern. Over the past several decades, the number of obese individuals throughout the United States has been on the rise. The 2017 reports from the Center for Disease Control and Prevention indicate that 39.8% of individuals 20 years and older, 93.3 million adults, in the United States were obese in 2015-2016, with an additional 31.8% considered overweight [7]. Over two-thirds of America's adult population struggles with being overweight and several other medical concerns linked to such status. Evidence has demonstrated a link between obesity, specifically increased levels of adiposity, and increased risk for several types of cancer including esophageal, colon, renal, liver, breast, pancreatic, ovarian, and prostate cancer [8, 9]. Additionally, obesity is associated with increased morbidity and mortality rates for cancer patients as compared to individuals of healthy weight [10, 11]. Based on a prostate cancer biopsy cohort study, obesity was also shown to be associated with higher-grade tumors [12]. Several studies have demonstrated that obesity does not specifically promote the development of prostate cancer; however, it does promote a more aggressive disease state [10]. In fact, a meta-analysis of about 11,000 prostate cancer patients revealed that patients who maintained a weight loss of at least 11 pounds over 10 years had a significantly lower risk for developing aggressive, high-grade prostate cancer [10, 13]. Additionally, obesity is linked to a higher rate of biochemical recurrence (increasing PSA levels) after prostate cancer treatment such as a prostatectomy or radiation [12]. Another study demonstrated, through meta-analysis, that biochemical recurrence of prostate cancer is positively correlated with excess body mass index (BMI) [14].

Obesity has been proposed to fuel prostate cancer in a variety of ways, including altered expression of biomolecules and genes and increased rates of basal-to-luminal cell differentiation within the prostate due to HFD induced inflammation [15-17]. One study suggests that excess white adipose tissue (WAT) in obese patients directly contributes to cancer progression [15]. The authors previously demonstrated that adipose stromal cells (ASCs) are released into the blood stream from WAT in obese patients and are further increased in cancer patients [15]. These ASCs contribute to the tumor-promoting microenvironment, supporting cell vascularization, promoting tumor growth, and a more aggressive disease state [15]. Cancer cells are known to release C-X-C motif ligand 1 (CXCL1) and C-X-C motif ligand 8 (CXCL8), and patients with prostate cancer have been shown to have increased CXCL1 expression. Human ASCs express C-X-C motif receptor 1 (CXCR1) and C-X-C motif receptor 2 (CXCR2) which serve as receptors CXCL1 and CXCL8 [15]. These receptors are drawn to the ligands produced by cancer cells, therefore bringing the ASCs close to the tumor where it can easily infiltrate the tumor and promote progression [15].

Another possible mechanism for obesity's contribution to progressive prostate cancer is through oxidized low-density lipoprotein/ lectin-like oxidized low-density lipoprotein receptor-1 (oxLDL/LOX-1) [16]. oxLDL, which serves as the ligand for LOX-1, has been found to be elevated in patients with advanced prostate cancer [16]. LOX-1 is associated with obesity and is overexpressed in metastatic prostate cancer [16]. When LOX-1 is activated by oxLDL, it promotes epithelial to mesenchymal transition, i.e. increasing mesenchymal markers and decreasing epithelial markers, in prostate cancer cells *in vitro*

[16]. This activation also causes restructuring of the cytoskeleton and induces migration of prostate cancer cells. The authors of this study also demonstrated *in vivo* that, in a nu/nu mouse xenograft model, LOX-1 was necessary for prostate tumor growth and, additionally, that it increased the tumorigenic potential in prostate cancer cells [16]. Another study demonstrated that a HFD promotes cellular proliferation within the prostate and formation of prostatic intraepithelial neoplasia in K14-Pten transgenic mice, which is considered a precursor to prostate cancer [17]. They also used mice to demonstrate that a HFD supports immune cell infiltration into prostate tissues, recruiting cytokines which can contribute to tumor growth [17]. Lastly, they demonstrated that a HFD can promote basal cell to luminal cell differentiation by way of inflammation, which again promotes prostate cancer progression [17].

Laurent et al. recently published data utilizing both *in vitro* and *in vivo* models, including cancer cell lines, murine models, and human tumor tissues. They demonstrated that adipocytes from the periprostatic adipose tissue promote migration of tumor cells [18]. Mature adipocytes secrete C-C motif chemokine ligand 7 (CCL7) which then travels through the periprostatic adipose tissue, into the prostate, where it then stimulates the migration of prostate cancer cells that express the C-C motif chemokine receptor (CCR3) [18]. It was found that obesity increased the concentration of CCL7 produced, which then aids in the extension of the tumor beyond the prostate gland and into the periprostatic adipose tissue [18]. Ultimately, these data reveal several potential mechanisms through which obesity may support aggressive prostate cancer and contributes to high-grade tumors.

Pigment Epithelium-Derived Factor

Cancer results from an accumulation of mutations in tumor suppressor genes and oncogenes. Pigment epithelium-derived factor (PEDF) is a tumor suppressor gene protein that is known to be down regulated in prostate cancer tissue as well as in the serum of prostate cancer patients when compared to healthy individuals [19-21]. PEDF is a 50 kDa endogenously secreted, multifunctional glycoprotein that was first discovered as a factor secreted by fetal retinal pigment epithelial (RPE) cells [22]. It has both secreted and intracellular pools. PEDF is expressed in many tissues and organs, with the highest expression in liver and adipose tissue, and can also be found circulating throughout the body in human serum [23]. PEDF was first shown to have neurotrophic effects, promoting survival of neurons, in the retina [24]. In 1999, it was confirmed that PEDF also has potent anti-angiogenic action directly on endothelial cells, inhibiting the growth of new blood vessels [25]. It was this discovery that first prompted the idea the PEDF might have therapeutic values. The anti-angiogenic activity of PEDF acts via suppression of proliferation and via induction of apoptosis in vascular endothelial cells [25]. In addition to these functions, the last quarter of a century of research has allowed for discovery of numerous other functions of PEDF including anti-tumor cell (anti-proliferative and/or pro-apoptotic), anti-inflammatory, anti-oxidation, and lipid metabolism regulatory functions [26].

The PEDF protein, encoded by the *Serpinf1* gene on human chromosome 17, consists of 418 amino acids forming three main beta-sheets and ten alpha-helices [27]. The name of the PEDF gene, *Serpinf1,* reflects its membership in the serine protease inhibitory superfamily,

commonly referred to as Serpins [23]. PEDF has the characteristic reactive center loop of all serpins; however, it does not exhibit the typical protease inhibitory properties [28]. Other Serpins, such as SerpinA4, are also known for their role in regulation of angiogenesis, similar to that of PEDF [29]. The PEDF protein has a unique asymmetrical charge distribution, one side being very acidic and the other being very basic [27]. Additionally, PEDF is known to have several protein binding sites, including sites for heparin [30] and collagen [31] binding. It is important to note that within the PEDF protein, two distinct functional peptides have been identified, a 34-mer and a 44-mer [23]. The 44-mer, residues 58-101, is recognized for its neurotrophic functions [32] and for its ability to bind to receptors on different neurons [33]. Recently, the 44-mer has also been shown to stimulate triglyceride lipolysis in cultured cardiomyocytes [34]. PEDF's 34-mer peptide, residues 24-37 [32], has the anti-tumor activity (anti-angiogenic/pro-apoptotic) [32].

Serpinf1 **Gene Regulation**

A protein with such diverse functions requires unique and extensive regulation. It is known that the *Serpinf1* gene contains a 200 base pair proximal promoter region immediately preceding the transcription start site [35]. A CAAT box is present at -43 and plays an important role in transcription as it serves as a binding site for transcription factors, including hepatocyte nuclear factors 4 (HNF4), upstream stimulatory factor 1 (USF), and CCAAT/Enhancer Binding Protein (CHOP) [35]. Using chromatin immunoprecipitation analysis and sequencing (ChIP-seq), researchers also located three microphthalmia-associated transcription factor (MITF) binding regions within the first intron of the *Serpinf1* gene in humans and in mice, two of which were highly conserved [36]. Another

enhancer box was found to be in the promoter of the human gene, about 1.3 kilobases upstream of the transcription start site [36]. They also demonstrated that the binding of MITF to these regions promotes transcription of the gene [37]. Additionally, nuclear receptor co-repressor (NCoR1) has been found to occupy the PEDF gene promoter in benign proliferating intestinal epithelial cells. NCoR1 represses gene expression, which allows the cells to continue to proliferate [38]. Intestinal epithelial cells with forced PEDF expression demonstrated slower proliferation rates, supporting NCoR1's regulatory function [30]. Also within the promoter region lays a cluster of *Alu* repetitive sequences [39]. These sequences are members of the short interspersed nuclear element sequences (SINES). Alu sequences have several different roles in transcription and post-transcription regulation. They are known to be CG-rich, making them an ideal target for DNA methylation, and also provide targets sites for miRNA in untranslated regions at the 3' end of genes [39]. A strong correlation between Alu elements and chromatin interactions, as well as functional DNA elements such as promoters and enhancers, has been established, supporting their regulatory function [39]. Additionally, they contain many general transcription factor-binding sites.

The p53 family of transcription factors, which includes p53, p63, and p73, plays a role in genetic regulation of PEDF in cancer. p53 is a well-known pro-apoptotic and anti-proliferative protein responsible for transcriptionally regulating many genes. It is found to be highly mutated in cancers, and it has been demonstrated that PEDF causes overexpression of p53 in lung cancer cell lines A549 and Calu-3, which accounts for PEDF's pro-apoptotic abilities [40]. While p53 does not appear to bind to the PEDF gene promoter,

response elements for p63 and p73 proteins are contained within the PEDF gene promoter [41], and another study has shown that p63 and p67 induce PEDF expression in human colorectal cancer cells [41]. Thus, p63 and p67 could promote the expression of PEDF, which in turn causes overexpression of p53 resulting in a blockage on cell proliferation and/or apoptosis. Surprisingly, however, p63 has been found to be upregulated in prostate cancer when compared to benign tissues, although it does exhibit an abnormal localization pattern with p63 dispersed throughout the cell and not strictly in the nucleus, suggesting it may not be functional [42].

Epigenetic regulation of *Serpinf1* is another potential mechanism of this gene's suppression in cancers. DNA hypermethylation of tumor suppressor genes has been linked to several cancer types[43]. The paired-like homeodomain 1 (*PITX1*) gene, a tumor suppressor gene, was found to be hypermethylated in esophageal squamous cell sarcoma when compared to normal tissues. This hypermethylation was significantly linked to tumor depth and advanced tumor stage [44]. Additionally, methylation of tissue factor pathway inhibitor 2 (*TFPI2),* another tumor suppression gene, was found to be significantly higher in both tumor tissues of gastric cancer and colorectal cancer, compared to healthy tissue [45]. Recently, hypermethylation of the *Serpinf1* gene promoter in prostate cancer tissues was also discovered at two separate sites denoted with GeneID numbers 517 and 5176 [46]. However, PEDF levels in the tissue were not assessed within this study, leaving it unclear if protein expression was affected due to this hypermethylation. Further studies need to be performed in order to determine how this DNA hypermethylation may alter PEDF expression in prostate cancer tissues.

PEDF and Prostate Cancer

PEDF can inhibit tumor growth and has been shown to cause tumor regression *in vitro* in human malignant glioma cells, ovarian cancer, melanoma, and prostate cancer [19, 47-49]. Decreased levels of PEDF have been found in human prostate cancer tissues, as compared to healthy tissue, correlating with a higher vascular density and tumor progression [19, 21, 50]. PEDF-deficient mice develop epithelial hyperplasia in the prostate, demonstrating PEDF's contribution to the inhibition of prostate epithelial tissue growth [19]. Additionally, this same study reveals that exogenous PEDF triggered apoptosis in prostate cancer cells *in vitro* [19]. Moreover, *in vivo* exogenous PEDF treatment also limited prostate tumor xenograft growth in nude mice by promoting endothelial apoptosis [19]. Utilizing androgen ablation treatment, via castration, PEDF expression in both prostatic rat tissues and human prostate cancer tissues, was increased [19]. These data demonstrate that PEDF is not mutated or deleted; thus, the decreased expression must be via another mechanism such as suppression of gene expression.

PEDF is found in two different pools within the body, intracellular and secreted. While several studies have verified that intracellular pools of PEDF are significantly lower in prostate cancer tissues [19], circulating levels of PEDF remain controversial. Two studies suggest that PEDF is significantly decreased in the serum of prostate cancer patients [51, 52]. In fact, one of these suggest that circulating PEDF may be a more accurate way to detect prostate cancer early when compared to methods such as a digital rectal exam or PSA [52]. However, a more recent study published in 2014 indicated that levels of PEDF in the serum were significantly higher in patients with prostate cancer than in healthy

individuals [53]. These authors concluded that PEDF levels within the serum can also be used for pathological analysis of the prostate tumor. Further studies will need to be conducted to determine prostate cancer's effects on PEDF expression within the serum of prostate cancer patients.

A recent study revealed that PEDF may also be beneficial in a combined therapy for mCRPC. This study examined two different taxane chemotherapies, cabazitaxel and docetaxel, currently utilized for symptomatic mCRPC as monotherpaies and then as part of a combination therapy with PEDF. They found that *in vitro*, cabazitaxel suppressed proliferation of CRPC cells with a higher efficacy than docetaxel. *In vivo*, when low doses of cabazitaxel combined with PEDF were administered to a CL1 CRPC xenograft mouse model, intermittent doses inhibited progression of the disease, preventing tumor migration and increasing activity of macrophages on the prostate cancer cells [54].

Furthermore, when considering obesity and prostate cancer, increased periprostatic fat tissue was found to be associated with more aggressive prostate cancer [55]. This specific study found that secretions from the periprostatic fat tissue removed from obese patients contained more pro-proliferative proteins than in periprostatic fat tissue from lean patients or even from subcutaneous fat tissues[56]. The authors concluded that obesity and increased periprostatic fat tissue stimulate prostate cancer progression. Another study suggests that this may be due to the periprostatic fat tissue serving as a source of interleukin-6, a cytokine that promotes tumor progression [56].

Interestingly, excess OA has been shown to suppress PEDF expression (Doll et al, unpublished observation). *In vitro*, oleic acid (OA) treatment (250-1000 μM) was used to simulate an obese microenvironment by inducing lipid overload in prostate cells. Three different prostate cancer cell lines were analyzed: LNCaP, DU145, and PC3, as well as an immortalized normal prostate epithelial cell line, RWPE-1. They observed that OA treatment results in significantly lower secreted PEDF levels in all cell lines, including RWPE-1 (Doll et al, unpublished observation). PEDF was also found to be significantly lower in cell lysate samples of OA-treated DU145 and PC3 cells which are the two androgen-independent, aggressive cell lines. This indicates that diet and obesity may play an important regulatory role in PEDF expression and disease progression, thus perhaps functioning as a nutrient sensor.

PEDF and Obesity

While our lab has demonstrated that an obese microenvironment suppresses secreted PEDF but does not effect on cellular concentrations, only a few other studies have examined PEDF expression in an obese microenvironment. Through *in vivo* analysis using mouse and rat models, increased PEDF expression in adipocytes and serum has been observed. With reduction of weight, PEDF levels were ultimately, reduced as well. In fact, they concluded that the increased PEDF expression in obese rodents played a crucial role in the development of obesity-induced insulin resistance [57]. Additional studies demonstrated similar findings in PEDF levels in serum of obese patients. One study previously demonstrated increased circulating PEDF levels in obese Caucasian men, with PEDF levels significantly decreasing with weight loss [58]. This study concluded that the

increased circulating PEDF was likely associated increased PEDF expression in human adipocytes during differentiation [58]. However, another study examined if PEDF in the liver or adipose may be associated with increased circulating PEDF linked to obesity-associated insulin resistance utilizing RT-PCR for mRNA levels and ELISA to analyze PEDF protein levels in the serum of obese patient samples. This study reported that the liver had a PEDF concentration of 2.09± 0.6 μg/ml while subcutaneous fat and visceral fat had lower levels at 1.18±0.38 μg/ml and 0.79±0.28 μg/ml respectively. Overall, they concluded that the liver was the likely source of the increased PEDF levels in the serum [59]. Another study found that mice fed a HFD did not have significantly different PEDF protein levels in the liver when compared to those fed a low fat chow measured by Western blot [57]. Overall, while there have been a few studies that have examined obesity's effect on PEDF expression, there is much more to still be explored.

DNA Methylation

DNA methylation is a chemical modification of DNA that is used to regulate gene expression by limiting access to the DNA promoter sequences, and, therefore, decreasing rates of transcription, which leads to decreased protein expression [60]. This process is extremely important as abnormal methylation patterns can lead to improper gene expression, which can result in serious diseases such as cancer. As mentioned above, hypermethylation of tumor suppressor genes is known to contribute to cancer progression; however, overall cancer cell genomes are hypomethylated, causing genomic instability and allowing expression of some oncogenes [61].

CpG islands (CGIs) are segments of DNA that contain clusters of CpG dinucleotides, a cytosine that precedes a guanine nucleotide in DNA. These regions are common in DNA, especially within the gene promoter regions, but they can also be found in other parts of the gene [62]. CGIs in gene promoters allow for gene silencing through DNA methylation. If the CGIs remain unmethylated, chromatin is structured such that it is easily accessible to RNA polymerases and transcriptional complexes [63]. However, methylation of CpG islands in gene promoters can hinder transcription factor binding to the promoter region, often causing decreased mRNA expression. Alternately, DNA methylation of CpG islands may induce alterations to the chromatin structure, totally restricting access to the gene, resulting in gene silencing [60, 63]. Inappropriate silencing of tumor suppressor genes facilitates cancer development and progression.

DNA methyltranferases (DNMTs) catalyze the covalent attachment of a methyl group onto the 5' position of the cytosine in CpG dinucleotide in DNA resulting in 5-methylcytosine (5mC). This process is cell cycle dependent and most often occurs during the S phase of the cell cycle, but it can also occur in the G2 and M phases [62]. There are three main DNMTs: DNMT1, DNMT3a, and DNMT3b. DNMT1 is the most common in adult cells and is considered the maintenance DNMT as it binds to hemi-methylated DNA and is responsible for methylating the newly synthesized strand of DNA. DNMT3a and DNMT3b are *de novo* methyltransferases and can bind to non-methylated DNA or hemi-methylated DNA. They are needed for early development after embryo implantation [64]. Truncated DNMT3b proteins cause abnormal DNA methylation patterns, altering gene expression, and are often found in cancer cells, specifically in leukemias [65].

DNA demethylase (MBD2) is known to carry out reverse action of the DNMTs, removing methyl groups from the DNA, working with the DNMTs in natural, reversible process [66]. One study proposed that DNMT activity is elevated, and DNA demethylase (MBD2) activity is decreased, in prostate cancer. They noted several relevant conclusions: (1) DNMT activity was two to three times higher in all cancer cell lines when compared the DNMT activity in the benign prostate epithelium cell line (BPH-1) and benign prostatic hyperplasia (BPH) tissue; (2) Specifically, DNMT1 protein expression was higher in all prostate cancer cell lines and tissues when compared to BPH-1 and BPH, with higher DNMT1 mRNA levels in prostate cancer cell lines compared to BPH-1; (3) There was no MBD2 activity in prostate cancer cell lines even though MBD2 activity was present in BPH-1 cells; and, (4) MBD2 protein expression was highest in BPH-1 cell lines, decreased in BPH cells, and absent in prostate cancer cells, and MBD2 mRNA expression was significant in all cell lines. In summary, they demonstrated the DNMT1 is significantly upregulated in prostate cancer cells, promoting hypermethylaton, and the activity of the demethylase must be altered at the transcriptional level [66].

Chemical inhibitors of DNMTs, specifically DNMT1, such as 5-aza-2-deoxycytidine (5-Aza-dC), have been approved by the FDA, after promising clinical trials, to be utilized for therapy of certain myeloid malignancies such as myelodysplastic syndromes, chronic melomonocytic leukemia, and acute myeloid leukemia [62, 67-69]. Additionally, as described earlier, hypermethylation of the *TFPI2* gene was found in both gastric tumor tissue and colorectal tumor tissue. The authors indicate that treatment of colorectal cancer

cell lines with 5-Aza-dC significantly increased the expression of *TFPI2* [45]. While 5-Aza-dC has been successfully used on prostate cancer cells *in vitro* to study methylation effects on genes such as *PMEPA1* and *GSTP1*, it has not been utilized to study the methylation of *Serpinf1* and is not an FDA approved drug for prostate cancer [70, 71].

There are two known mechanisms by which 5-Aza-dC inhibits DNMT1 activity. The first is considered a passive mechanism. 5-Aza-dC, an analog of cytosine, is able to replace cytosines in newly synthesized DNA strands. Once 5-Aza-dC residues become incorporated into the replicated DNA, DMNT1 attempts to methylate the 5-Aza-dC residues. However, due to the structure of 5-Aza-dC, the DMNT1s are unable to do so and become trapped at the 5-Aza-dC residue, preventing continued methylation by that enzyme [60, 62]. The success of 5-Azd-C in this passive mechanism is dependent on the cell cycle, and it has been shown that a slower DNA replication phase, the S phase of the cell cycle, increases the efficiency 5-Aza-dC due to this passive mechanism of entrapping DMNT1 [62, 72]. The more time spent in the replication phase, the more DMNT1 proteins are entrapped by 5-Aza-dC residues, leading to lower levels of DNA methylation. The second mechanism is the active mechanism; 5-Aza-dC induces degradation of DMNT1 via the proteasome pathway, decreasing DNMT1 levels and, thus, decreasing DNA methylation [60, 72]. This pathway is dependent on DNA synthesis because 5-Aza-dC must be incorporated into the DNA in order for the DNMT1 to attack and trigger its degradation [60].

DNA Methylation and Obesity

Obesity and HFDs have been shown to affect gene expression through epigenetic regulation, specifically by DNA methylation. One study revealed that CpG islands in obese individuals are more prone to DNA methylation than healthy weight control individuals [73]. Another study located 31 CpGs in DNA from whole blood cells in obese children that were differentially methylated, most hypermethylated, compared to those in non-obese children [74]. When the authors analyzed 151 regions that were differentially methylated in severely obese children, they found that many of these genes are also found in cancer pathways [74]. They note that childhood obesity could lead to differentially methylated DNA which could increase one's risk for cancer later in life [74]. In mice, a HFD altered hepatic gene expression of several proteins, including hypermethylation of Pleckstrin Homology Like Domain Family A Member 1 (*Phlda1)* which is responsible for regulating apoptosis and angiogenesis, as well as Forkhead Box A1 (*Foxa1),* and Forkhead Box A2 (*Foxa2),* which both regulate lipid homeostasis [75]. Levels of adiponectin, a protein secreted from the adipose tissue that has a variety of functions including inhibiting prostate cancer cell proliferation, have been found to be significantly decreased in serum levels of patient's with progressive prostate cancer [76]. In this study, the authors demonstrated that *in vitro* treatment of LNCaP with 5-Aza-dC and Trichostatin A (TSA), a deacetylation enzyme, resulted in increased expression of adiponectin where adiponectin was previously absent [76]. Furthermore, with bisulfite sequencing analysis, they found that the expression of this hormone is decreased via hypermethylation of the gene's promoter [76]. These data support that DNA hypermethylation is a prevalent mechanism of gene regulation in an obese microenvironment.

Current work has shown decreased expression of PEDF *in vitro* in an obese microenvironment in both normal prostate epithelial and in prostate cancer cell lines. PEDF expression in an obese microenvironment *in vivo* must be explored. Therefore, here, I utilized dietary studies and genetic differences in mice to analyze PEDF levels in an obese microenvironment.

HYPOTHESIS AND SPECIFIC AIMS

The central hypothesis of this study was that an obese microenvironment regulates *Serpinf1*gene expression in normal prostate, liver, and periprostatic adipose tissue. This hypothesis was addressed in two specific aims:

Specific aim 1: Determine if an obese or high fat microenvironment suppresses PEDF expression in prostatic tissue in mice *in vivo*.

Working hypothesis: High fat diet-fed and genetically obese mice will have decreased PEDF expression in the prostate tissue as compared to lean mice.

Specific aim 2: Determine if an obese or high fat microenvironment regulates PEDF expression in liver and periprostatic fat tissue in mice *in vivo*.

Working hypothesis: High fat diet-fed and genetically obese mice will have increased PEDF expression in the liver tissue, and decreased expression in the periprostatic fat tissue, as compared to lean mice.

Through these studies, I will determine if an obese microenvironment results in suppression of PEDF *in vivo*. This data will allow for progressive future studies regarding PEDF expression in obese prostate cancer microenvironments and the underlying mechanisms that may result in any differences.

MATERIALS AND METHODS

Mice strains and dietary treatment

All mouse studies and procedures have been approved by the Institutional Animal Care and Use Committee (IACUC) of the University of Wisconsin-Milwaukee. Two mouse experiments were performed using with C57BL/6 background strain of mice as listed in **Table 1**. This plan provided two different models for obesity. The first model is the consumption of a HFD compared to a normal, healthy control diet (CD), and the second model is a genetic model, ob/ob mice, which have a null mutation in the leptin gene, which causes over-eating and alters metabolism resulting in significant weight gain [77]. For the first model, wild-type mice were randomly assigned to either the CD (n=24) or the HFD (n=24). The CD was a low glycemic diet with 16.8% kcal from fat (Envigo, TD.120455). This diet contains 3.3 Cal/g of food [78]. The HFD was an adjusted calories diet with 60.3% kcal from fat (Envigo, TD.06414). This contains 5.1 Cal/g of food [78] (Table 1). For experiment 2, the wild-type (n=24) and ob/ob (n=24) mice were fed the standard lab diet (Table 1).

Table 1. Treatment Groups for Aims 1 and 2

Experiment 1:				**Experiment 2:**		
Treatment Group	**Mouse strain**	**Diet**		**Treatment Group**	**Mouse strain**	**Diet**
1 – control	Wild-	Harlan		1	Wild-	Harlan

diet	type	TD.120455 (16.8% kcal from fat)			type	TD.7912 (17% kcal from fat)
2 – high fat diet	Wild-type	Harlan TD.06414 (60% kcal from fat)		2	Ob/ob	Harlan TD.7912 (17% kcal from fat)

These diets were initiated at 8 weeks of age and were sustained for 16 weeks. The mice were then euthanized at 6 months of age. Mice were housed 4 to a cage. For the CD versus HFD model, food intake, as well as mouse weights, were monitored and recorded weekly throughout the study. Using 24 mice per treatment group allows for n=8 for each tissue analysis of protein for these studies, and mRNA and DNA for future studies.

Mouse tissue dissection

Isoflurane was used to anaesthetize the mice. After administration of the anesthesia, blood was collected, for future experiments, and the mice received additional anesthesia to induce death. A cervical dislocation was used to ensure death prior to dissection. With the mice in a dorsal position, scissors and forceps were used to create midline incision through the abdomen and two lateral incisions between the paws without penetrating the peritoneum. Subcutaneous adipose tissue was then collected. Next, an incision was then made through the peritoneum. The gonadal fat pads and liver were collected. The intestines were pushed upwards and the entire periprostatic fat and all 3 lobe of the prostate (ventral, right and left dorsolateral, and anterior) were collected using a dissecting scope. The prostate tissues were weighed prior to being placed in individual cyrovials. All

tissue samples were flash frozen in liquid nitrogen, and then stored at -80°C until processing.

Sample Processing

Tissue homogenization: Tissue samples were removed from -80°C and placed on ice. Prostate tissues were removed from cryovial and weighed then placed in a 1.7 mL microfuge tube. The liver and periprostatic fat tissue had to be cut and portioned prior to being weighed. The quantity of tissue extraction reagent was calculated using the total tissue weight. Tissue extraction reagent (Invitrogen, Carlsbad, CA) was prepared by adding 1 X Protease Inhibitor Cocktail (Sigma-Aldrich, St. Louis, MO) and PMSF (Sigma-Aldrich, St. Louis, MO). The appropriate volume of prepared tissue extraction reagent solution was added to each microfuge tube. Tissues were then homogenized using a motor and disposable pestle while kept on ice. After homogenization, samples were incubated on ice for at least 5 minutes then centrifuged at 14,000 RPM for 5 minutes. The supernatant was collected using a pipet and long tips, ensuring to avoid any pellet or floating debris (floating debris occurs in the adipose tissue samples). The sample was placed in a 0.5 mL siliconized centrifuge tube and stored at 4°C for use in the following days.

Analysis of samples

Coomassie Protein Assay*:* Total protein content in each tissue sample was quantified using a standard Coomassie dye-binding assay. Eight standards were prepared with prediluted standards (Thermo Fisher Cat. #23208) with final concentrations of 0 µg/mL, 25 µg/mL, 125 µg/mL, 250 µg/mL, 500 µg/mL, 750 µg/mL, 1000 µg/mL, and 1500 µg/mL. In separate

microcentrifuge tubes, 490 µL aliquots of Coomassie reagent (Thermo Fisher Cat. #1856209) were mixed with 10 µL of each prediluted standard. Prostate tissue samples, and most periprostatic fat samples, required a 1:20 dilution, so 0.5 µL of the prostate tissue homogenate was added to 490 µL of Coomassie reagent and 9.5 µL of PBS. Liver tissue samples were diluted 1:50. Ten µL of the diluted sample was added to 490 µL of Coomassie reagent. Samples were incubated for 5 minutes. For each standard and sample, 225 µL was transferred in duplicate into a 96 well plate and then read using a Synergy HT plate reader (Biotek, Winooski, VT) at 595 nm. Protein concentration from the each sample was calculated from the standard curve.

Enzyme-linked immunosorbent assay (ELISA): The concentration of PEDF protein in each tissue homogenate sample was measured with an ELISA (MyBioSource, Mouse PEDF ELISA Kit) following the manufacturer's protocol. Calculations were done prior to ELISA preparation using the protein concentration results from the Coomassie assay. Initially, a dilution of test samples were used to identify an appropriate total protein concentration to use in the assay for each tissue type. From these trials, it was determined that 0.5 µg/well of total protein from each sample should be utilized to determine PEDF concentration. All reagents were prepared per the manufacturer's instructions. One mL of Sample Diluent was added to the Standard vial. The vial was placed on an orbital rotator to gently disturb the solution and ensure complete dissolution. Serial dilutions were performed with the standard creating standards with concentrations of 0 ng/mL, 0.16 ng/mL, 0.32 ng/mL, 0.63 ng/mL, 1.25 ng/mL, 2.5 ng/mL, 5 ng/mL, and 10 ng/mL. Samples were prepared using volumes calculated previously and any necessary dilutions were prepared using the sample

diluent. Once all standards and samples were prepared, 100 µL of each standard and sample was loaded onto the ELISA plate in duplicate. The plate was sealed and was placed in the incubator at 37°C, 5% CO_2, for 2 hours. After 2 hours, the ELISA plate was removed and liquid was aspirated from each well. Then, 100 µL of Detection Solution A was added to each well using a multichannel pipet. The plate was covered and placed in incubator for 1 hour. Next, the solution from each well was aspirated and filled with wash buffer. Wash buffer remained in wells for at least one minute prior to being aspirated. The wash was repeated two more times for a total of three washes, blotting dry after the last wash. Next, 100 µL of Detection Solution B was added to each well. The plate was covered and incubated for another hour. The plate was washed for a total of five times, then blotting dry. Then, 90 µL of Substrate Reagent was added to each well. The plate was again covered and placed in the incubator for 15 minutes. The plate sealer was removed and 50 µL of Stop Solution was added to each well. The plate was then read at 450 nm using the Synergy HT plate reader (Biotek, Winooski, VT). The unknown concentration in each tissue sample was calculated from the standard curve.

Data Analysis: The results of these assays were then analyzed for statistical significance using a student t-test with a significance level of 0.05. Aim 1 results examined the differences in prostate tissues while aim 2 results examined PEDF levels in liver and periprostatic fat. A one-way ANOVA was used to analyze the differences in total PEDF concentration among the three different prostate lobes.

RESULTS

Specific aim 1: Determine if an obese or high fat microenvironment suppresses PEDF expression in prostatic tissue in mice *in vivo*.

Food consumption and weight gain in wild-type mice on HFD versus CD.

While the ob/ob mouse model is well characterized with regard to weight gain and food consumption [79], HFD models vary with the actual HFD versus CD used in the study. The CD was a low glycemic diet with 16.8% kcal from fat and 3.3 Cal/g of food [78]. The HFD was an adjusted calories diet with 60.3% kcal from fat and 5.1 Cal/g of food [78]. All animals were weighed weekly and food consumption was measured per cage of mice weekly. The average amount of food consumed per mouse per week was calculated (Figure 1A). Mice on the HFD on average consumed signifcantly less gram weight of food each week than mice on the CD (Figure 1B; P-value = 6.691×10^{-12}).

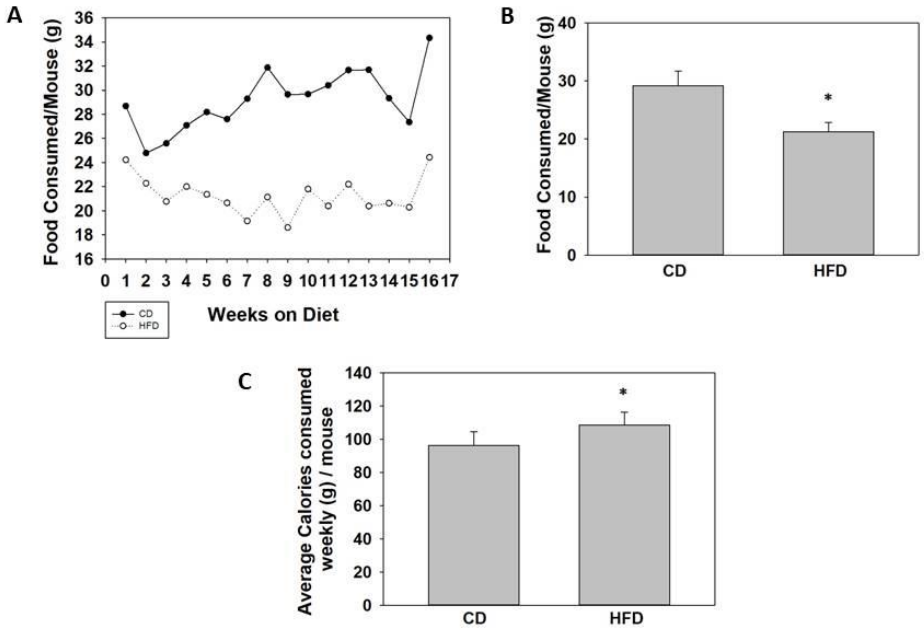

Figure 1. High fat diet mice consumed significantly less food as compared to wild-type mice. Wild-type C57Bl/6 mice were fed a control diet (CD) (n=24), a low glycemic diet with 16.8% kcal from fat (Envigo, TD.120455), or a high fat diet (HFD) (n=24), an adjusted Calories diet with 60.3% kcal from fat (Envigo, TD.06414) for 16 weeks beginning at 8 weeks of age. Each week, the amount of food consumed (g) was measured then divided 4, the number of mice in each cage, to determine the average amount of food consumed per mouse. **(A)** demonstrates the average amount of food consumed per mouse over time. **(B)** shows the end point food consumption data and that mice on the high fat diet consumed significantly less food than mice on the control diet (*P-value = 6.691×10^{-12}). **(C)** shows the average amount of calories consumed weekly per mouse. The control diet contains 3.3 Cal/g and the high fat diet contained 5.1 Cal/g. When comparing the total average Calories consumed per mouse on each diet, the endpoint data was used, and the mice on the high fat diet consumed significantly more calories (*P-value = 0.000196).

However, the HFD contained 5.1 Cal/g of food while the CD contained 3.3 Cal/g of food. Thus, when analyzing the food consumed by Calories, the mice on the HFD consumed signifcantly more Calories than the mice on the CD (Figure 1C; P-value = 0.000196), as expected.

The increased Calorie consumption thus explains why the HFD mice gained significantly more weight over the 16 week diet when compared to the mice on the CD (Figure 2; P-

value = 1.995 x 10^{-14}). The mice on the HFD, on average, had a 93.3% weight gain over time while the mice on the CD experienced a 51% increase in weight over time (Figure 2B; P-value = 1.995 x 10^{-14}).

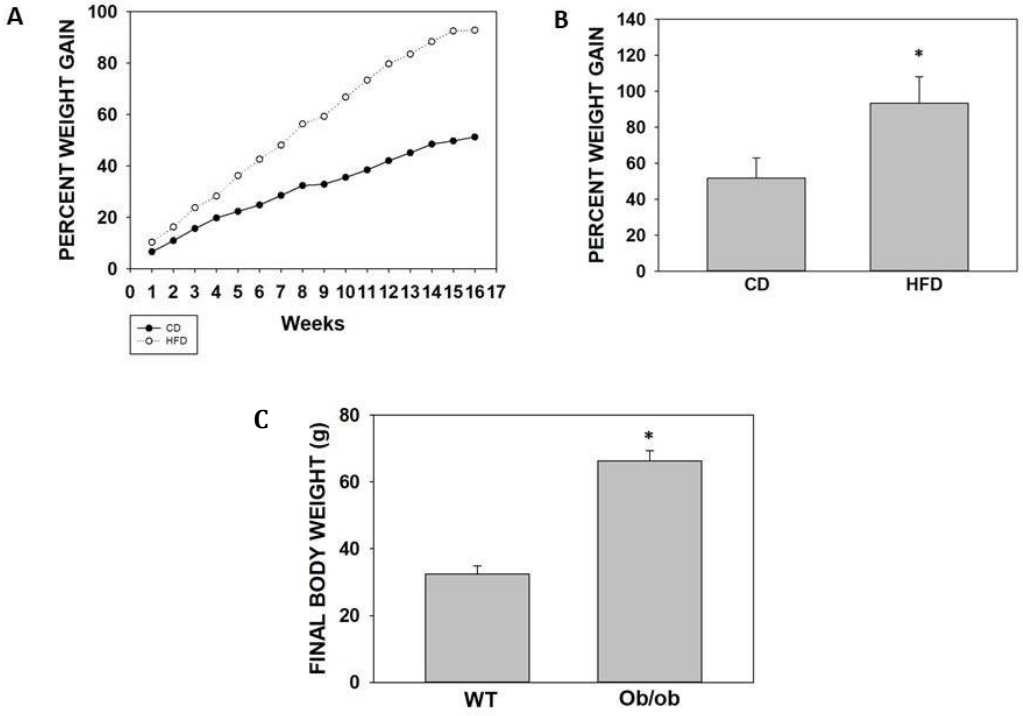

Figure 2. Mice weight gain in dietary studies. Wild-type C57Bl/6 mice were fed a control diet (n=24), a low glycemic diet with 16.8% kcal from fat (Envigo, TD.120455), or a high fat diet (n=24), an adjusted calories diet with 60.3% kcal from fat (Envigo, TD.06414) for 16 weeks beginning at 8 weeks of age. Mice were weighed weekly. **(A)** Shows the average percent of weight gain per mouse per week on each diet. **(B)** Shows the overall average end weight gain per mouse on each diet *(P-value = 1.995 x 10^{-14}). **(C)** Wild-type mice C57Bl/6 mice and ob/ob mice were fed the standard laboratory chow. They began the diet at 8 weeks of age and the diet was sustained for 16 weeks. Final body weights were taken at the end of the diet, when mice were 24 weeks old (*P-value=8.631 x 10^{-39}).

Prostatic PEDF Levels.

With the HFD study mice, when examining the PEDF concentrations in the prostate tissue homogenates, no significant difference was found in either the ventral, anterior, or dorsolateral prostate samples between the two diet groups (Figure 3).

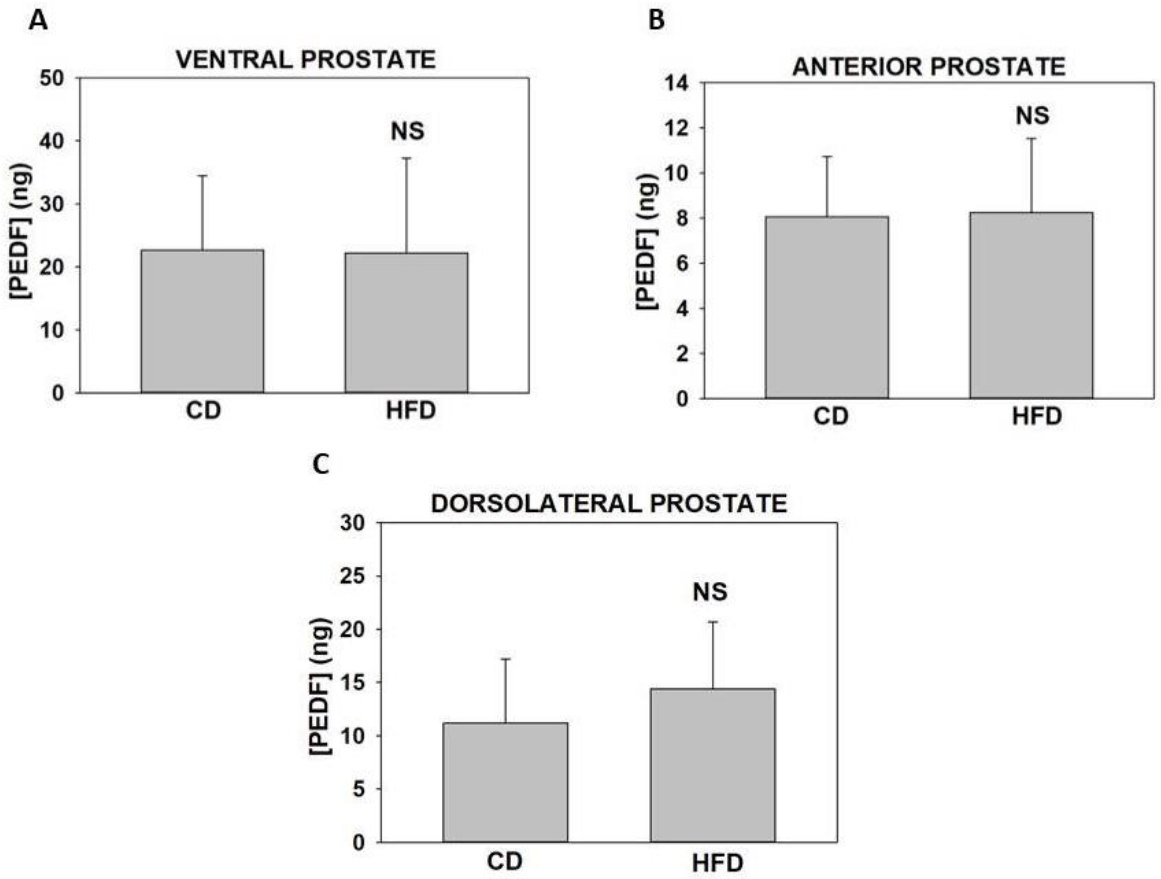

Figure 3. High fat diet did not alter PEDF levels in the ventral, anterior, or dorsolateral prostate tissues. Prostate tissues were collected from **w**ild-type C57Bl/6 mice on a control diet (CD) (n=8), a low glycemic diet with 16.8% kcal from fat (Envigo, TD.120455), or a high fat diet (HFD) (n=8), a diet with 60.3% kcal from fat (Envigo, TD.06414). Tissues were homogenized and protein levels were quantified with a Coomassie protein assay. An ELISA (MyBioSource) was performed to quantify PEDF protein in 0.5 µg of total protein. The prostate lobes are **(A)** Ventral prostate (P-value = 0.824); **(B)** Anterior prostate (P-value = 0.903); and, **(C)** Dorsolateral prostate (P-value = 0.312). **NS**, non-significant.

In the prostate tissue homogenates collected from wild-type and ob/ob mice on a standard laboratory diet, no difference in PEDF levels were observed in the ventral (Figure 4A) or

dorsolateral (Figure 4B) samples. However, PEDF levels were significantly lower in the anterior prostate samples in the ob/ob mice compared to the wild-type mice (Figure 4C).

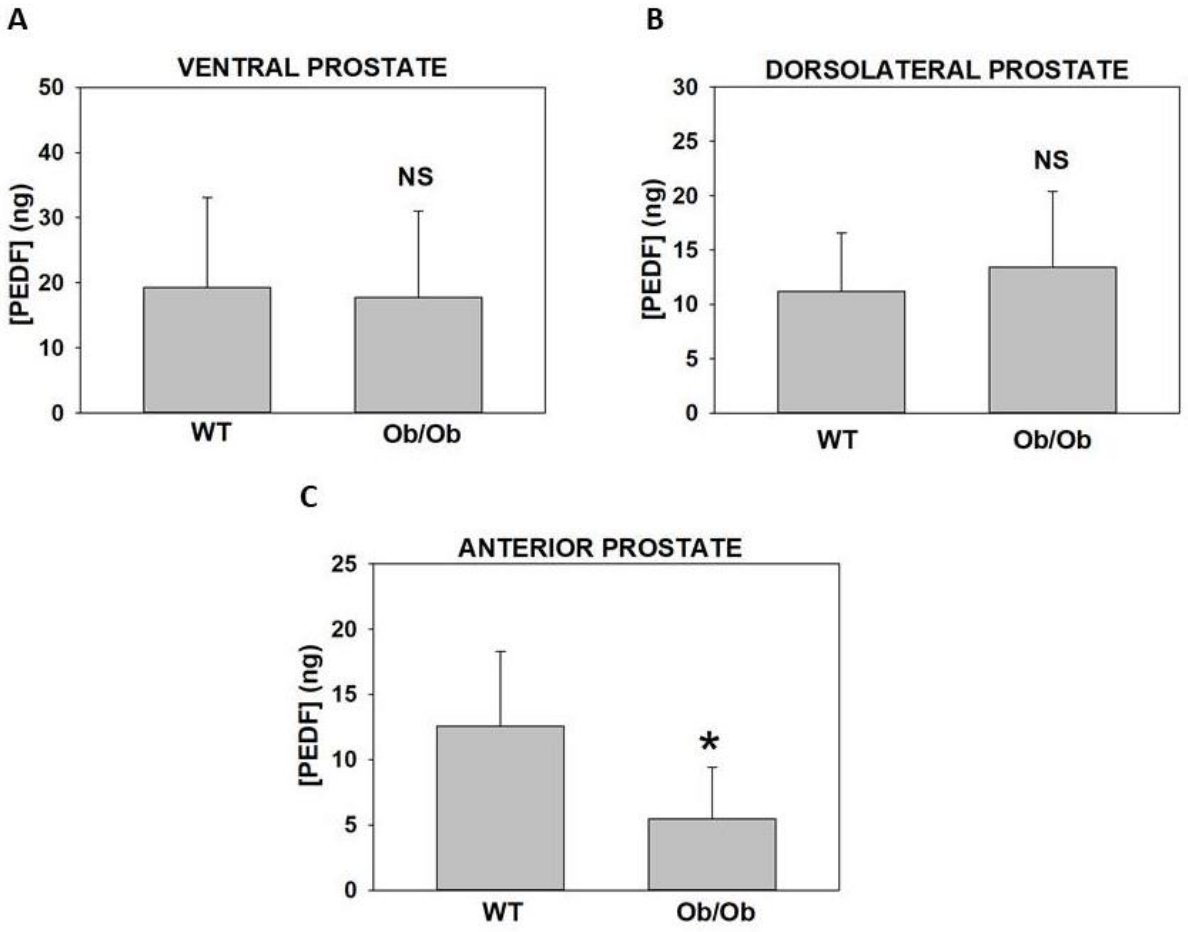

Figure 4. PEDF levels in ventral, anterior, and prostate tissues in wild-type (WT) versus ob/ob mice on a standard laboratory diet. Prostate tissues were collected from **w**ild-type C57Bl/6 mice (n=8) or ob/ob C57Bl/6 mice (n=8) on a standard laboratory diet. Tissues were homogenized and protein levels were quantified with a Coomassie protein assay. An ELISA (MyBioSource) was performed to quantify PEDF protein, in 0.5 µg of total protein, in the **(A)** Ventral prostate (P-value = 0.951); **(B)** Dorsolateral prostate (P-value = 0.477); and, **(C)** Anterior prostate (P-value = 0.0163). **NS**, non-significant.

Interestingly, PEDF levels varied between lobes. To date, PEDF protein levels have not previously been quantified in the mouse prostate. In both studies, the ventral prostate tissues in the control mice produced approximately twice as much PEDF than the anterior

prostate and dorsolateral prostate. The ventral prostate tissue in the WT control mice had significantly more PEDF (*P-value = 0.003) than the anterior or dorsolateral prostate tissues. However, due to large variance in samples, the WT mice on the standard laboratory diet showed no significant difference (P-value = 0.0190) (Figure 5).

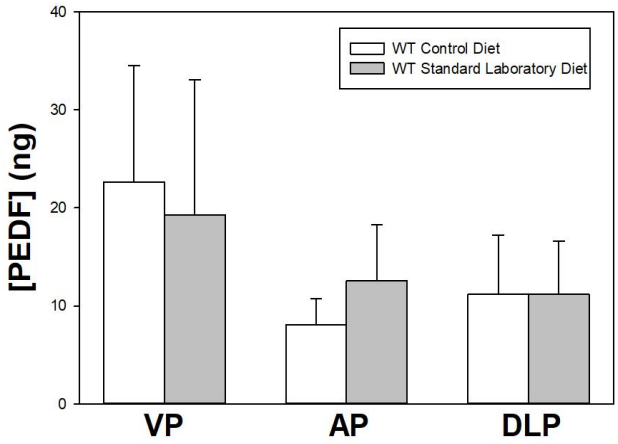

Figure 5. PEDF levels vary by prostate lobe in control mice. Prostate tissues were collected from **w**ild-type C57Bl/6 mice on a control diet or standard laboratory diet (n=8). Diets began when mice were 8 weeks of age and they remained on the diet for 16 weeks prior to tissue collection. Tissues were homogenized and protein levels were quantified with a Coomassie protein assay. An ELISA (MyBioSource) was performed to quantify PEDF protein in 0.5 µg of total protein. PEDF levels in the ventral prostate appear to be approximately twice as high as high as the levels in the anterior and dorsolateral prostate. One-way ANOVA analysis among the wild-type prostate tissues from the control diet showed no significant difference (P = 0.003). One-way ANOVA analysis among the wild-type prostate tissues from the standard laboratory diet prostate tissues showed no significant difference (P = 0.190).

Specific aim 2*:* Determine if an obese or high fat microenvironment suppresses PEDF expression in liver and periprostatic fat tissue in mice *in vivo.*

Wild-type mice on HFD versus CD.

A previous study in human tissue showed that PEDF expression in the liver increases with obesity while a mouse HFD study showed no significant difference [57, 59]. Some studies propose that this increase in PEDF expression in the liver, rather than changes in the

adipose tissue, may result in the increased circulating PEDF levels, seen in obese patients [59] . This study's analysis of liver tissue of wild-type mice on a CD versus HFD demonstrated no significant difference in PEDF levels (Figure 6). Similarly to the prostatic tissues, again, no significant changes in PEDF levels were observed in periprostatic adipose tissues (Figure 7). This study is also the first to report PEDF levels in periprostatic fat tissue.

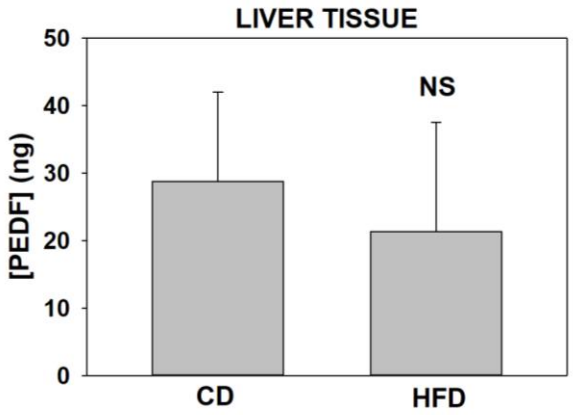

Figure 6. PEDF levels were not significantly different in liver tissue homogenates from wild-type (WT) mice on a control diet (CD) versus a high fat diet (HFD). Liver tissues were collected from **w**ild-type C57Bl/6 mice on a control diet (n=6), a low glycemic diet with 16.8% kcal from fat (Envigo, TD.120455), or a high fat diet (n=7), an adjusted calories diet with 60.3% kcal from fat (Envigo, TD.06414). Diets were started at 8 weeks of age and mice remained on the diet for 16 weeks prior to collection of tissues. Tissues were homogenized and protein levels were quantified with a Coomassie protein assay. An ELISA (MyBioSource) was performed to quantify PEDF protein in 0.5 µg of total protein (P-value = 0.390). **NS**, non-significant.

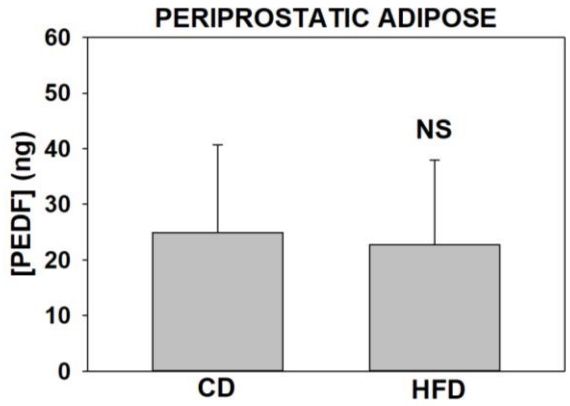

Figure 7. PEDF levels were not significantly different in periprostatic adipose tissue homogenates from wild-type (WT) mice on a control diet (CD) versus a high fat diet (HFD). Periprostatic adipose tissues were collected from **w**ild-type C57Bl/6 mice on a control diet (n=8), a low glycemic diet with 16.8% kcal from fat (Envigo, TD.120455), or a high fat diet (n=7), an adjusted calories diet with 60.3% kcal from fat (Envigo, TD.06414). Diets were started at 8 weeks of age and mice remained on the diet for 16 weeks prior to collection of tissues. Tissues were homogenized and protein levels were quantified with a Coomassie protein assay. An ELISA (MyBioSource) was performed to quantify PEDF protein in 0.5 µg of total protein (P-value = 0.784). **NS**, non-significant.

Wild-type mice versus ob/ob mice on standard laboratory diet.

With the liver tissues collected from the wild-type mice and ob/ob mice, on a standard laboratory diet, multiple ELISAs were performed utilizing different protein levels; however, with each protein concentration for both wild-type and ob/ob, all absorbances were above range of the standard curve. Thus, PEDF levels in these tissues were not obtained. With the periprostatic adipose tissue, no significant difference was observed in PEDF levels between the wild-type mice and ob/ob mice on a standard laboratory diet (Figure 8), though levels between two mouse studies are in the same range (Figures 7 and 8).

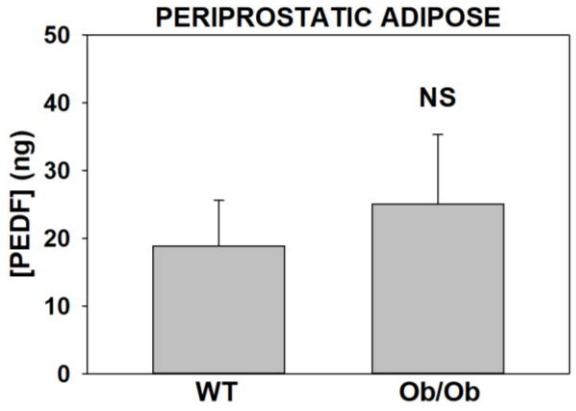

Figure 8. PEDF levels were not significantly different in periprostatic adipose tissue homogenates in wild-type (WT) mice versus ob/ob mice on a standard laboratory diet. Periprostatic adipose tissues were collected from wild-type C57Bl/6 mice (n=6) or ob/ob C57Bl/6 mice (n=6) on a standard laboratory diet. Tissues were homogenized and protein levels were quantified with a Coomassie protein assay. An ELISA (MyBioSource) was performed to quantify PEDF protein in 0.5 µg of total protein (P-value = 0.244). **NS**, non-significant.

DISCUSSION AND CONCLUSIONS

PEDF is an anti-angiogenic, anti-tumorigenic protein, which has been found to be down regulated in human prostate cancer tissue as compared to healthy tissue [19, 50]. Additionally in prostate cancer, obesity and HFDs have been associated with higher-grade tumors and a more aggressive disease state [10, 12]. The Doll lab has previously examined dietary effects on PEDF expression *in vitro* using an OA treatment model to simulate an obese microenvironment in a normal epithelial cell line and in prostate cancer cell lines by inducing lipid overload (Doll lab, unpublished observation). They found that the obese microenvironment suppressed secreted PEDF protein expression in all cell lines and suppressed intracellular PEDF expression in the two androgen-independent cell lines tested. However, prostatic PEDF levels have not been previously examined *in vivo* in normal or obese microenvironments. Thus, this study specifically explored the effects of

two obesity models, a HFD and genetic obesity (ob/ob mice), on PEDF protein expression in prostate, liver, and periprostatic fat tissue as compared to wild-type control mice.

In the HFD model, no differences in PEDF expression were found in the ventral, anterior, and dorsolateral prostate tissues (Figure 3). However, in the ob/ob model, a difference was observed in the anterior prostate lobe only, with significantly less PEDF (Figure 4C). No differences in the ventral prostate or dorsolateral prostate lobes were observed in this model (Figure 4A, 4B). This study did, however, establish that PEDF levels may be nearly twice as high in the ventral prostate tissues when compared to the anterior prostate or dorsolateral prostate samples. PEDF levels were significantly higher in the ventral prostate tissues in WT mice on the CD when compared to the anterior and dorsolateral prostate tissues. However, in the ob/ob model, statistical significance was not achieved but a similar trend is apparent (Figure 5). The differences in PEDF levels among the prostate lobes may be due to anatomical and histological differences.

The dorsolateral lobe of the prostate in mice shares many anatomical and mRNA expression signatures with the human PZ zone of the prostate. It is in the PZ zone that 75-85% of prostate adenocarcinomas occur. The dorsolateral lobe is composed of small acini lined with epithelial cells with several infoldings [80]. The anterior lobe is most similar to the CZ zone in humans which accounts for about 25% of the prostate tissue. In mice it is also known as the coagulating gland. This lobe has more complex acini, usually appearing with a cribriform pattern which looks like small holes. The luminal space is lined with columnar epithelial cells and typically contains secretions of inflammatory and

immunoregulatory proteins generated by eosinophils [80]. The ventral prostate lobe is not considered analogous to any human prostate zone. It typically consists of many large acini lined with simple or cuboidal epithelial cells with a flat luminal border [80]. Though PEDF secretory patterns from each lobe have not been established, research does indicate that the different lobes secrete unique proteins. One analysis demonstrates that the dorsolateral and anterior prostate lobes typically secrete a protein similar to the immunoglobulin-binding protein, immunoglobulin-binding protein-like protein, experimental autoimmune prostatitis antigen protein 2, glucose-regulated protein 78, and a few others [81]. The ventral prostate lobe secretes a spermine-binding protein, a hypothetical scavenger receptor, as well as serine protease inhibitor Kazal type-3 [81]. Importantly, our study is the first to report PEDF levels in prostate tissue *in vivo* in normal and HFD/obese microenvironments, specifically, protein levels in the different mouse prostate lobes.

While there is general agreement that the ob/ob model is obese, a clear definition of obesity in the HFD model has not been established. While the HFD method is often used to induce obesity in mice [79, 82], there are no set parameters to characterize an obese mouse from a lean mouse, unlike the BMI system used on humans. Collecting mouse weights weekly demonstrated that both groups gained weight over the 16 weeks, and the mice on the HFD did gain significantly more weight as expected. However, we cannot clearly conclude that the mice on the HFD were truly obese since no clear definition exists in mice. During these experiments, literature-based research by others in the lab determined that gonadal fat pad weight is the best estimate, other than DEXA scan, to estimate the percent of body fat was by the weight of the gonadal fat pad (Doll lab, unpublished data). The mean

gonadal fat pad weights for the control and HFD groups were 1.183 g and 2.554 g respectively (*P-value = 0.0000409). Whine in the ob/ob model, the gonadal fat pad weights for the wild-type and ob/ob mice on the standard laboratory diet were 0.501 and 1.887 respectively (*P-value = 0.000000660).With the HFD, the gonadal fat pad weight is reflective of weight gain. In the genetically obese mice, gonadal fat pad weight was not as indicative of body weight. However, the control diet differed between the two models which may contribute to the differences observed. Thus, future *in vivo* studies should utilize this method. However, a cutoff point of gonadal fat pad weight, to designate obesity, has not been established in the scientific literature.

From these studies, it does not appear that an obese microenvironment decreases PEDF expression in normal prostate tissue. Though, there is variability between samples in all of the ELISA data. While, each treatment group had a sample size of n=6-8, because this is the first report, the high variance was not anticipated. Increasing the sample size of each group may reduce the size of error and would be necessary to firmly establish that no differences exist. To determine how many mice would be needed to determine if difference exists, a power analysis should be performed based on the data of this study.

Though no difference was observed in healthy tissue, the same cannot be assumed in a tumor microenvironment. While a healthy microenvironment works to achieve functional homeostasis and protect again unwanted pathogens, a tumor microenvironment can alter tissue and cellular function, ultimately supporting the development of more advanced tumors [83]. This can be caused by many different factors including suppression of tumor

suppressor genes or increased expression of oncogenes for example. Research indicates that adipose tissue is associated with cancer [83]. Therefore, an obese microenvironment may in fact alter the expression of PEDF in an already compromised tumorigenic microenvironment.

With previous studies showing that PEDF is significantly decreased in prostate cancer cells, and the fact that obesity is linked to more aggressive prostate tumors, the effects of an obese microenvironment on PEDF levels should be assessed in a prostate tumor model. Additionally, there are no published studies on prostatic PEDF levels in prostate cancer patients that stratify the patients by an obesity measure (i.e. BMI or waist circumference).

The role of adiposity in prostate cancer progression has been examined in many studies. Obesity often results in subclinical inflammation. A recent study of men recently diagnosed with prostate cancer revealed that periprostatic WAT inflammation was present in nearly 50% of the cases and it was also significantly associated with factors such as BMI, Gleason score, and larger adipocyte size [84]. Another study revealed that increased periprostatic fat tissue was found to be associated with more aggressive prostate cancer [55]. Laurent et al. recently published findings *in vitro* and *in vivo* studies utilizing cancer cell lines, murine models, and human tumors to study how obesity effects prostate cancer [18]. They demonstrated that adipocytes from the periprostatic adipose tissue promote migration of prostate tumor cells *in vitro* in migration assays [18]. Another study found that secretions collected *ex vivo* from the periprostatic fat tissue from obese patients contained more pro-proliferative proteins than in periprostatic fat tissue from lean patients or even from

subcutaneous fat tissues. The authors concluded that secretions from obese periprostatic adipose tissue stimulate prostate cancer cell proliferation [56].

In this study, neither obesity model demonstrated differences in PEDF levels in periprostatic adipose tissue when compared to control groups. Again, there appears to be large variability of PEDF protein in the periprostatic adipose samples in each treatment group. A 2009 study found PEDF expression to be 3 times higher in gonadal fat tissue in mice on a HFD relative to those on a low-fat chow and about 2.5 times greater in ob/ob mice when compared to the control [57]. These studied analyzed PEDF levels with a mouse PEDF ELISA kit from Chemicon International and utilized a low-fat control diet (4% fat), while in our study, we used PEDF ELISA kits from MyBioSource and a CD of 16.8% kcal from fat. This suggests that different adipose tissue depots respond differently to HFD/obese environments. Due to the variance in PEDF levels, increasing the sample size to verify that there is indeed no significant difference in PEDF levels in the periprostatic adipose tissue from an obese microenvironment compared to the control as well as in other tissue types would be advised. A power analysis with the data obtained in this study should be performed prior to determine how many mice should be used in each treatment to determine if a difference exists.. In addition, the length of the diet may also need to be increased to ensure sufficient time for a truly obese microenvironment to be established.

Several studies have examined circulating PEDF with regard to obesity-related diseases, including diabetes and insulin-resistance. One study previously demonstrated increased circulating PEDF levels in obese Caucasian men, with PEDF levels significantly decreasing with weight loss [58]. This study concluded that the increased circulating

PEDF was likely associated increased PEDF expression in human adipocytes during differentiation [58]. However, another study examined if PEDF in the liver or adipose may be associated with increased circulating PEDF linked to obesity-associated insulin resistance utilizing RT-PCR for mRNA levels and ELISA to analyze PEDF protein levels in the serum of obese patient samples. This study reported that the liver had a PEDF concentration of 2.09± 0.6 μg/ml while subcutaneous fat and visceral fat had lower levels at 1.18±0.38 μg/ml and 0.79±0.28 μg/ml respectively. Overall, they concluded that the liver was the likely source of the increased PEDF levels in the serum [59]. Another study found that mice fed a HFD did not have significantly different PEDF protein levels in the liver when compared to those fed a low fat chow measured by Western blot [57]. Due to these inconsistencies, PEDF levels in the liver in an obese microenvironment were analyzed in this study. In our HFD obesity model, no significant difference in PEDF levels was found in the liver tissue of mice.

While we did not see statistically significant differences in these experiments, differences could still be present at the protein modification level. PEDF has at least two known isoforms with different molecular weights and charges referred to as PEDF-1 and PEDF-2, and these are thought to result from post-translational modification [26, 85]. One study demonstrates that PEDF-2 carried out anti-tumor functions while PEDF-1 exhibited very minimal effects [85]. It is possible that the PEDF is still present but modified in a manner that leaves it potentially less, or not, functional with regard to its anti-tumor properties. Future studies using Western blot or mass spectrometry to analyze PEDF protein samples in prostate, liver, and adipose tissues, may identify changes in the PEDF isoforms present in the samples with the HFD/obesity.

FUTURE DIRECTIONS

Overall, the data obtained did not support the hypothesis that an obese microenvironment would alter PEDF levels in prostate, liver, or adipose tissue *in vivo.* While *in vitro* studies have shown PEDF suppression in both a normal prostate epithelial cell line, RWPE-1, and in prostate cancer cell lines (LNCaP, DU145, and PC-3), these are the first studies to examine PEDF levels *in vivo* in the prostate and under a HFD or obese microenvironment. If the same *in vivo* experiments are to be repeated, increasing the number of mice per treatment group may reduce variability and assist in confirming that no difference is present. As stated above, a power analysis should be performed utilizing the data from this study in order to determine how many mice will be needed for future studies to determine if there is a difference between the two groups. Additionally, the diet regiment should be reevaluated. Although mice on the HFD did gain significantly more weight, perhaps the mice were not on the diet long enough, or did not gain enough fat mass, to suppress PEDF protein levels in the prostate. Additionally, similar *in vivo* experiments can be performed using Western blot or mass spectrometry to analyze PEDF protein isoforms in prostate, liver, and adipose tissue from obese microenvironments to determine if there is potentially a change in the PEDF protein isoform present in the tissue. Additionally, PEDF expression in prostate tissue should be evaluated in an obese tumor microenvironment. A tumor environment has altered gene expression, gene function, and tissue function, so analyzing how obesity may support the compromised environment and overall effect PEDF expression is important. All in all, further investigation is required to fully understand how an obese microenvironment effects PEDF expression *in vivo.*

REFERENCES

1. *Prostate Cancer Treatment (PDQ(R)): Health Professional Version*, in *PDQ Cancer Information Summaries*2002: Bethesda (MD).

2. *Key Statistics for Prostate Cancer*. 2017; 2017:[Available from: https://www.cancer.org/cancer/prostate-cancer/about/key-statistics.html.

3. de Brot, S., et al., *Regulation of vascular endothelial growth factor in prostate cancer.* Endocr Relat Cancer, 2015. **22**(3): p. R107-23.

4. Ahmed, A., S. Ali, and F.H. Sarkar, *Advances in androgen receptor targeted therapy for prostate cancer.* J Cell Physiol, 2014. **229**(3): p. 271-6.

5. Salinas, C.A., et al., *Prostate cancer in young men: an important clinical entity.* Nat Rev Urol, 2014. **11**(6): p. 317-23.

6. Lin, D.W., M. Porter, and B. Montgomery, *Treatment and survival outcomes in young men diagnosed with prostate cancer: a Population-based Cohort Study.* Cancer, 2009. **115**(13): p. 2863-71.

7. Prevention, C.f.D.C.a. *National Center for Health Statistics: Obesity and Overweight*. May 3, 2017; Available from: https://www.cdc.gov/nchs/fastats/obesity-overweight.htm.

8. Byers, T. and R.L. Sedjo, *Body fatness as a cause of cancer: epidemiologic clues to biologic mechanisms.* Endocr Relat Cancer, 2015. **22**(3): p. R125-34.

9. Vucenik, I. and J.P. Stains, *Obesity and cancer risk: evidence, mechanisms, and recommendations.* Ann N Y Acad Sci, 2012. **1271**: p. 37-43.

10. Alshaker, H., et al., *Leptin signalling, obesity and prostate cancer: molecular and clinical perspective on the old dilemma.* Oncotarget, 2015. **6**(34): p. 35556-63.

11. Calle, E.E., et al., *Overweight, obesity, and mortality from cancer in a prospectively studied cohort of U.S. adults.* N Engl J Med, 2003. **348**(17): p. 1625-38.

12. De Nunzio, C., et al., *The uncertain relationship between obesity and prostate cancer: an Italian biopsy cohort analysis.* Eur J Surg Oncol, 2011. **37**(12): p. 1025-9.

13. Allott, E.H., E.M. Masko, and S.J. Freedland, *Obesity and prostate cancer: weighing the evidence.* Eur Urol, 2013. **63**(5): p. 800-9.

14. Hu, M.B., et al., *Obesity has multifaceted impact on biochemical recurrence of prostate cancer: a dose-response meta-analysis of 36,927 patients.* Med Oncol, 2014. **31**(2): p. 829.

15. Zhang, T., et al., *CXCL1 mediates obesity-associated adipose stromal cell trafficking and function in the tumour microenvironment.* Nat Commun, 2016. **7**: p. 11674.

16. Gonzalez-Chavarria, I., et al., *LOX-1 activation by oxLDL triggers an epithelial mesenchymal transition and promotes tumorigenic potential in prostate cancer cells.* Cancer Lett, 2017. **414**: p. 34-43.

17. Kwon, O.J., et al., *High fat diet promotes prostatic basal-to-luminal differentiation and accelerates initiation of prostate epithelial hyperplasia originated from basal cells.* Stem Cell Res, 2016. **16**(3): p. 682-91.

18. Laurent, V., et al., *Periprostatic adipocytes act as a driving force for prostate cancer progression in obesity.* Nat Commun, 2016. **7**: p. 10230.

19. Doll, J.A., et al., *Pigment epithelium-derived factor regulates the vasculature and mass of the prostate and pancreas.* Nat Med, 2003. **9**(6): p. 774-80.

20. Qingyi, Z., et al., *Unfavorable prognostic value of human PEDF decreased in high-grade prostatic intraepithelial neoplasia: a differential proteomics approach.* Cancer Invest, 2009. **27**(7): p. 794-801.

21. Rivera-Perez, J., et al., *Evaluation of VEGF and PEDF in prostate cancer: A preliminary study in serum and biopsies.* Oncol Lett, 2018. **15**(1): p. 1072-1078.

22. Tombran-Tink, J. and L.V. Johnson, *Neuronal differentiation of retinoblastoma cells induced by medium conditioned by human RPE cells.* Invest Ophthalmol Vis Sci, 1989. **30**(8): p. 1700-7.

23. Sagheer, U., J. Gong, and C. Chung, *Pigment Epithelium-Derived Factor (PEDF) is a Determinant of Stem Cell Fate: Lessons from an Ultra-Rare Disease.* J Dev Biol, 2015. **3**(4): p. 112-128.

24. Becerra, S.P., et al., *Pigment epithelium-derived factor behaves like a noninhibitory serpin. Neurotrophic activity does not require the serpin reactive loop.* J Biol Chem, 1995. **270**(43): p. 25992-9.

25. Dawson, D.W., et al., *Pigment epithelium-derived factor: a potent inhibitor of angiogenesis.* Science, 1999. **285**(5425): p. 245-8.

26. He, X., et al., *PEDF and its roles in physiological and pathological conditions: implication in diabetic and hypoxia-induced angiogenic diseases.* Clin Sci (Lond), 2015. **128**(11): p. 805-23.

27. Simonovic, M., P.G. Gettins, and K. Volz, *Crystal structure of human PEDF, a potent anti-angiogenic and neurite growth-promoting factor.* Proc Natl Acad Sci U S A, 2001. **98**(20): p. 11131-5.

28. Steele, F.R., et al., *Pigment epithelium-derived factor: neurotrophic activity and identification as a member of the serine protease inhibitor gene family.* Proc Natl Acad Sci U S A, 1993. **90**(4): p. 1526-30.

29. Sun, H.M., et al., *SERPINA4 is a novel independent prognostic indicator and a potential therapeutic target for colorectal cancer.* Am J Cancer Res, 2016. **6**(8): p. 1636-49.

30. Alberdi, E.M., J.E. Weldon, and S.P. Becerra, *Glycosaminoglycans in human retinoblastoma cells: heparan sulfate, a modulator of the pigment epithelium-derived factor-receptor interactions.* BMC Biochem, 2003. **4**: p. 1.

31. Meyer, C., L. Notari, and S.P. Becerra, *Mapping the type I collagen-binding site on pigment epithelium-derived factor. Implications for its antiangiogenic activity.* J Biol Chem, 2002. **277**(47): p. 45400-7.

32. Filleur, S., et al., *Two functional epitopes of pigment epithelial-derived factor block angiogenesis and induce differentiation in prostate cancer.* Cancer Res, 2005. **65**(12): p. 5144-52.

33. Bilak, M.M., et al., *Identification of the neuroprotective molecular region of pigment epithelium-derived factor and its binding sites on motor neurons.* J Neurosci, 2002. **22**(21): p. 9378-86.

34. Zhang, H., et al., *PEDF and PEDF-derived peptide 44mer stimulate cardiac triglyceride degradation via ATGL.* J Transl Med, 2015. **13**: p. 68.

35. Xu, X., et al., *Molecular phylogeny of the antiangiogenic and neurotrophic serpin, pigment epithelium derived factor in vertebrates.* BMC Genomics, 2006. **7**: p. 248.

36. Dadras, S.S., et al., *A novel role for microphthalmia-associated transcription factor-regulated pigment epithelium-derived factor during melanoma progression.* Am J Pathol, 2015. **185**(1): p. 252-65.

37. Fernandez-Barral, A., et al., *Regulatory and functional connection of microphthalmia-associated transcription factor and anti-metastatic pigment epithelium derived factor in melanoma.* Neoplasia, 2014. **16**(6): p. 529-42.

38. Doyon, G., et al., *Nuclear receptor co-repressor is required to maintain proliferation of normal intestinal epithelial cells in culture and down-modulates the expression of pigment epithelium-derived factor.* J Biol Chem, 2009. **284**(37): p. 25220-9.

39. Gu, Z., et al., *Enrichment analysis of Alu elements with different spatial chromatin proximity in the human genome.* Protein Cell, 2016. **7**(4): p. 250-66.

40. Li, L., et al., *Pigment epithelial-derived factor (PEDF)-triggered lung cancer cell apoptosis relies on p53 protein-driven Fas ligand (Fas-L) up-regulation and Fas protein cell surface translocation.* J Biol Chem, 2014. **289**(44): p. 30785-99.

41. Sasaki, Y., et al., *Identification of pigment epithelium-derived factor as a direct target of the p53 family member genes.* Oncogene, 2005. **24**(32): p. 5131-6.

42. Dasen, B., et al., *T-cadherin in prostate cancer: relationship with cancer progression, differentiation and drug resistance.* J Pathol Clin Res, 2017. **3**(1): p. 44-57.

43. Jones, P.A. and S.B. Baylin, *The epigenomics of cancer.* Cell, 2007. **128**(4): p. 683-92.

44. Otsubo, T., et al., *DNA hypermethyation and silencing of PITX1 correlated with advanced stage and poor postoperative prognosis of esophageal squamous cell carcinoma.* Oncotarget, 2017. **8**(48): p. 84434-84448.

45. Hu, H., et al., *The role of TFPI2 hypermethylation in the detection of gastric and colorectal cancer.* Oncotarget, 2017. **8**(48): p. 84054-84065.

46. Kobayashi, Y., et al., *DNA methylation profiling reveals novel biomarkers and important roles for DNA methyltransferases in prostate cancer.* Genome Res, 2011. **21**(7): p. 1017-27.

47. Guan, M., et al., *Inhibition of glioma invasion by overexpression of pigment epithelium-derived factor.* Cancer Gene Ther, 2004. **11**(5): p. 325-32.

48. Cheung, L.W., et al., *Pigment epithelium-derived factor is estrogen sensitive and inhibits the growth of human ovarian cancer and ovarian surface epithelial cells.* Endocrinology, 2006. **147**(9): p. 4179-91.

49. Abe, R., et al., *Overexpression of pigment epithelium-derived factor decreases angiogenesis and inhibits the growth of human malignant melanoma cells in vivo.* Am J Pathol, 2004. **164**(4): p. 1225-32.

50. Halin, S., et al., *Decreased pigment epithelium-derived factor is associated with metastatic phenotype in human and rat prostate tumors.* Cancer Res, 2004. **64**(16): p. 5664-71.

51. Oon, S.F., et al., *The identification and internal validation of a preoperative serum biomarker panel to determine extracapsular extension in patients with prostate cancer.* Prostate, 2012. **72**(14): p. 1523-31.

52. Byrne, J.C., et al., *2D-DIGE as a strategy to identify serum markers for the progression of prostate cancer.* J Proteome Res, 2009. **8**(2): p. 942-57.

53. Ide, H., et al., *Circulating pigment epithelium-derived factor (PEDF) is associated with pathological grade of prostate cancer.* Anticancer Res, 2015. **35**(3): p. 1703-8.

54. Jarvis, C., et al., *Cabazitaxel regimens inhibit the growth of prostate cancer cells and enhances the anti-tumor properties of PEDF with various efficacy and toxicity.* Prostate, 2018. **78**(12): p. 905-914.

55. Venkatasubramanian, P.N., et al., *Periprostatic adipose tissue from obese prostate cancer patients promotes tumor and endothelial cell proliferation: a functional and MR imaging pilot study.* Prostate, 2014. **74**(3): p. 326-35.

56. Finley, D.S., et al., *Periprostatic adipose tissue as a modulator of prostate cancer aggressiveness.* J Urol, 2009. **182**(4): p. 1621-7.

57. Crowe, S., et al., *Pigment epithelium-derived factor contributes to insulin resistance in obesity.* Cell Metab, 2009. **10**(1): p. 40-7.

58. Sabater, M., et al., *Circulating pigment epithelium-derived factor levels are associated with insulin resistance and decrease after weight loss.* J Clin Endocrinol Metab, 2010. **95**(10): p. 4720-8.

59. Moreno-Navarrete, J.M., et al., *Liver, but not adipose tissue PEDF gene expression is associated with insulin resistance.* Int J Obes (Lond), 2013. **37**(9): p. 1230-7.

60. Patel, K., et al., *Targeting of 5-aza-2'-deoxycytidine residues by chromatin-associated DNMT1 induces proteasomal degradation of the free enzyme.* Nucleic Acids Res, 2010. **38**(13): p. 4313-24.

61. Cheung, H.H., et al., *DNA methylation of cancer genome.* Birth Defects Res C Embryo Today, 2009. **87**(4): p. 335-50.

62. Desjobert, C., et al., *Combined analysis of DNA methylation and cell cycle in cancer cells.* Epigenetics, 2015. **10**(1): p. 82-91.

63. Deaton, A.M. and A. Bird, *CpG islands and the regulation of transcription.* Genes Dev, 2011. **25**(10): p. 1010-22.

64. Jin, B. and K.D. Robertson, *DNA methyltransferases, DNA damage repair, and cancer.* Adv Exp Med Biol, 2013. **754**: p. 3-29.

65. Ostler, K.R., et al., *Cancer cells express aberrant DNMT3B transcripts encoding truncated proteins.* Oncogene, 2007. **26**(38): p. 5553-63.

66. Patra, S.K., et al., *DNA methyltransferase and demethylase in human prostate cancer.* Mol Carcinog, 2002. **33**(3): p. 163-71.

67. Piekarz, R.L. and S.E. Bates, *Epigenetic modifiers: basic understanding and clinical development.* Clin Cancer Res, 2009. **15**(12): p. 3918-26.

68. Yang, X., et al., *Targeting DNA methylation for epigenetic therapy.* Trends Pharmacol Sci, 2010. **31**(11): p. 536-46.

69. Ramos, M.P., et al., *DNA demethylation by 5-aza-2'-deoxycytidine is imprinted, targeted to euchromatin, and has limited transcriptional consequences.* Epigenetics Chromatin, 2015. **8**: p. 11.

70. Sharad, S., et al., *Methylation of the PMEPA1 gene, a negative regulator of the androgen receptor in prostate cancer.* Epigenetics, 2014. **9**(6): p. 918-27.

71. Chiam, K., et al., *GSTP1 DNA methylation and expression status is indicative of 5-aza-2'-deoxycytidine efficacy in human prostate cancer cells.* PLoS One, 2011. **6**(9): p. e25634.

72. Kress, C., H. Thomassin, and T. Grange, *Active cytosine demethylation triggered by a nuclear receptor involves DNA strand breaks.* Proc Natl Acad Sci U S A, 2006. **103**(30): p. 11112-7.

73. Rhee, J.K., et al., *DNA Methylation Profiles of Blood Cells Are Distinct between Early-Onset Obese and Control Individuals.* Genomics Inform, 2017. **15**(1): p. 28-37.

74. Fradin, D., et al., *Genome-Wide Methylation Analysis Identifies Specific Epigenetic Marks In Severely Obese Children.* Sci Rep, 2017. **7**: p. 46311.

75. Zhang, P., et al., *DNA methylation alters transcriptional rates of differentially expressed genes and contributes to pathophysiology in mice fed a high fat diet.* Mol Metab, 2017. **6**(4): p. 327-339.

76. Tan, W., et al., *Adiponectin as a potential tumor suppressor inhibiting epithelial-to-mesenchymal transition but frequently silenced in prostate cancer by promoter methylation.* Prostate, 2015. **75**(11): p. 1197-205.

77. *Mouse Strain Datasheet - 000632*. 2018 [cited 2018; Available from: https://www.jax.org/strain/000632

78. Envigo. *Diet Induced Obesity*. Available from: https://www.envigo.com/products-services/teklad/laboratory-animal-diets/custom-research/diet-induced-obesity/.

79. Lutz, T.A. and S.C. Woods, *Overview of animal models of obesity.* Curr Protoc Pharmacol, 2012. **Chapter 5**: p. Unit5 61.

80. Oliveira, D.S., et al., *The mouse prostate: a basic anatomical and histological guideline.* Bosn J Basic Med Sci, 2016. **16**(1): p. 8-13.

81. Fujimoto, N., et al., *Identification of prostatic-secreted proteins in mice by mass spectrometric analysis and evaluation of lobe-specific and androgen-dependent mRNA expression.* J Endocrinol, 2006. **190**(3): p. 793-803.

82. Ji, W., et al., *Effects of canagliflozin on weight loss in high-fat diet-induced obese mice.* PLoS One, 2017. **12**(6): p. e0179960.

83. Wang, M., et al., *Role of tumor microenvironment in tumorigenesis.* J Cancer, 2017. **8**(5): p. 761-773.

84. Gucalp, A., et al., *Periprostatic adipose inflammation is associated with high-grade prostate cancer.* Prostate Cancer Prostatic Dis, 2017. **20**(4): p. 418-423.

85. Subramanian, P., et al., *Identification of pigment epithelium-derived factor protein forms with distinct activities on tumor cell lines.* J Biomed Biotechnol, 2012. **2012**: p. 425907.